Journal of Sound and Vibration 329 (2010) 687–699

Contents lists available at ScienceDirect

Journal of Sound and Vibration

journal homepage: www.elsevier.com/locate/jsvi

The effects of coupling and bubble size on the dynamical-systems behaviour of a small cluster of microbubbles

K.J.Y. Chong [a], C.Y. Quek [a], F. Dzaharudin [a], A. Ooi [a,*], R. Manasseh [b]

[a] Department of Mechanical Engineering, University of Melbourne, VIC 3010, Melbourne, Australia
[b] Fluid Dynamics Group, CSIRO Materials Science and Engineering, PO Box 56, Highett, VIC 3190, Melbourne, Australia

ARTICLE INFO

Article history:
Received 17 February 2009
Received in revised form
20 September 2009
Accepted 27 September 2009
Handling Editor: L.G. Tham
Available online 25 October 2009

ABSTRACT

This study endeavours to apply a theoretical model for predicting the dynamics of a bubble cluster of various sizes, within which each bubble may assume different initial conditions from other bubbles in the cluster. The resulting system of coupled Keller–Miksis–Parlitz equations are solved numerically, and the effects of coupling and bubble size on bubble cluster dynamics are examined for a given set of ultrasound parameters. It has been found that the effects of coupling are significant, and a bubble cluster's bifurcation characteristics and route to chaos can be altered by inter-bubble interactions. This gives rise to the possibility of suppressing the chaotic oscillations of microbubbles by varying bubble cluster size. Small equilibrium radii bubbles have little influence on the dynamics of neighbouring bubbles in a cluster via coupling. Furthermore, a bubble system consisting of smaller-sized bubbles transitions from order to chaos at lower driving pressure amplitudes.

1. Introduction

Since ultrasound driven microbubbles hold great potential in reshaping the boundaries of biomedical acoustics, numerous attempts have been made to investigate the dynamics of microbubbles. The classical Rayleigh–Plesset equation [1,2] forms a starting point for any theoretical investigation made into the realm of bubble dynamics. The Rayleigh–Plesset equation produces realistic results for large bubbles exposed to small to moderate forcing amplitudes. However, when the amplitude of bubble oscillations is large, particularly at the onset of cavitation, the results of numerical simulations have been found to yield little agreement with experimental data [3]. To account for this discrepancy, Keller and Miksis [3] have included the effects of acoustic radiation losses in the momentum conservation equation of a single bubble. The resulting Keller–Miksis equation has been adapted by Parlitz et al. [4] with slight modification to simplify the analysis of bubble dynamics during cavitation.

To accurately simulate the dynamics of a bubble system, the dynamics of every single bubble in the bubble cluster would have to be traced. Due to the significant amount of computational time involved in solving the set of governing nonlinear ordinary differential equations (ODEs) corresponding to every single bubble in the cluster, especially when the number of bubbles is large, many studies on the dynamics of a bubble cluster in the past were reduced to an examination of the dynamics of a single isolated bubble, subjecting that bubble to initial conditions and parameters which was an average value of the entire bubble system, and fully ignoring the effect of its interactions with neighbouring bubbles [5]. However, recent studies [6–10] have demonstrated that when inter-bubble distances in a cluster are small, the effects of coupling

* Corresponding author.
E-mail address: a.ooi@unimelb.edu.au (A. Ooi).

0022-460X/$ - see front matter © 2009 Elsevier Ltd. All rights reserved.
doi:10.1016/j.jsv.2009.09.037

between the bubbles can be significant. Efforts have been made by Ooi and Manasseh [11] to incorporate the effects of coupling in their investigation of bubble structure dynamics without incurring additional computational time. In keeping up with the aim of solving only a single ODE, the following assumptions have been adopted: (i) all bubbles have the same initial radii, (ii) all bubbles are subject to the same external pressure field and (iii) every single bubble are equidistant from each other. The adoption of the latter assumption, however, limits the foregoing analysis to a bubble cluster consisting of four bubbles at most.

It is the aim of this study to develop a theoretical model for predicting the dynamics of a bubble cluster without being limited to the aforementioned assumptions. The resulting system of coupled Keller–Miksis–Parlitz equations is solved for the dynamics of every single bubble in a cluster, and the effects of coupling and bubble size on the dynamical behaviour of bubble clusters will be investigated.

In this study, the dynamical behaviour of bubble clusters will also be examined in terms of the bubble bifurcation characteristics and route to chaos, as chaos is strongly linked to the onset of bubble inertial cavitation [12]. Lauterborn is one of the pioneers in applying the methods of chaos physics to bubble acoustics research [13]. Stroboscopic maps, based on a mapping of bubble wall velocity to bubble radius after every forcing period, have been used extensively by researchers such as [4] to assess the state of order or chaos of the bubble-acoustic dynamical system concerned. A collection of stroboscopic maps at different ultrasound parameters have also been used by these researchers to produce bifurcation diagrams, powerful tools in providing an insight on the inherently rich, nonlinear characteristics of the system, as well as detailing the order-to-chaos transition pathway of the system. Thus far, all these studies have been conducted on only a single bubble in isolation.

Allen et al. [14], Garbin et al. [15], MacDonald and Gomatam [16] and Takahira et al. [17] are examples of studies on the bifurcation characteristics of bubble clusters involving bubbles of different initial radii. The latter two studies concluded that when bubbles of different radii oscillate, inter-bubble interactions suppress the independent oscillations of each bubble such that all bubbles in the cluster take on collective behaviour. However, there is no investigation into how a large bubble affects the oscillation of smaller neighbouring bubbles and vice versa, and how this degree of influence varies as bubble size changes. The present study is therefore also motivated by the need to investigate how changing bubble equilibrium size and number of bubbles in a cluster could potentially affect the bifurcation characteristics and route to chaos of a group of bubbles.

2. Theoretical model for a bubble cluster

An equation of Keller–Miksis–Parlitz form is given by [4],

$$\ddot{R}=\frac{1}{\left(1-\frac{\dot{R}}{c}\right)R+\frac{4\mu}{\rho c}}\left[-\frac{\dot{R}^2}{2}\left(3-\frac{\dot{R}}{c}\right)-\frac{2\sigma}{\rho R}-\frac{4\mu\dot{R}}{\rho R}+\left(1+(1-3\kappa)\frac{\dot{R}}{c}\right)\left(\frac{P_0-P_v}{\rho}+\frac{2\sigma}{\rho R_0}\right)\left(\frac{R_0}{R}\right)^{3\kappa}\right.$$
$$\left.-\left(1+\frac{\dot{R}}{c}\right)\frac{P_0-P_v+\alpha\sin(2\pi f_{\mathrm{ext}}t)}{\rho}-\frac{2\pi f_{\mathrm{ext}}R\alpha}{\rho c}\cos(2\pi f_{\mathrm{ext}}t)\right] \quad (1)$$

where $R(t)$, R_0, μ, ρ, κ, c, σ, α and f_{ext} represent the instantaneous bubble radius, equilibrium bubble radius, dynamic viscosity of the liquid, density of liquid, polytropic exponent for bubble gas, speed of sound in air, surface tension of bubble wall, acoustic pressure amplitude and driving frequency respectively. The parameter values of $\mu=0.001\,\mathrm{kg\,m^{-1}s^{-1}}$, $\kappa=1.33$, $c=1484\,\mathrm{m\,s^{-1}}$, $\sigma=0.0725\,\mathrm{N\,m^{-1}}$, $P_v=2330\,\mathrm{Pa}$, $P_0=100,000\,\mathrm{Pa}$ for bubbles in water at 20 °C would be used for all simulations in this paper [3].

When a bubble cluster is considered, Eq. (1) can be applied to every single bubble in the cluster. To include the effects of coupling, a coupled-oscillator approximation for linearly coupled pairs of bubbles proposed by [18] can be used, in which case a coupling term of the form:

$$P_{si}=\sum_{j\neq i}^{N_{\mathrm{bub}}}\frac{1}{s_{ij}}(R_j^2\ddot{R}_j+2R_j\dot{R}_j^2) \quad (2)$$

would be added to the right hand side of Eq. (1). P_{si} represents the incremental pressure/density acting on bubble i due to pressure scattered by neighbouring bubbles in a cluster, R_j is the instantaneous radius of the jth neighbouring bubble, s_{ij} is the distance between the ith and jth bubble and N_{bub} is the number of bubbles in the cluster. Adopting the assumptions that the bubbles remain spherical throughout and the surrounding liquid is incompressible [18,19], the resulting equation becomes:

$$\ddot{R}_i=\frac{1}{\left(1-\frac{\dot{R}_i}{c}\right)R_i+\frac{4\mu}{\rho c}}\left[-\frac{\dot{R}_i^2}{2}\left(3-\frac{\dot{R}_i}{c}\right)-\frac{2\sigma}{\rho R_i}-\frac{4\mu\dot{R}_i}{\rho R_i}+\left(1+(1-3\kappa)\frac{\dot{R}_i}{c}\right)\left(\frac{P_0-P_v}{\rho}+\frac{2\sigma}{\rho R_{0i}}\right)\left(\frac{R_{0i}}{R_i}\right)^{3\kappa}\right.$$

$$-\left(1+\frac{\dot{R}_i}{c}\right)\frac{P_0-P_v+\alpha\sin(2\pi f_{\text{ext}}t)}{\rho}-\sum_{j\neq i}^{N_{bub}}\frac{1}{s_{ij}}\left(R_j^2\ddot{R}_j+2R_j\dot{R}_j^2\right)-\frac{2\pi f_{\text{ext}}R_i\alpha}{\rho c}\cos(2\pi f_{\text{ext}}t)\Bigg] \tag{3}$$

where R_i is the instantaneous radius of the ith bubble and R_{0i} is the equilibrium radius of the ith bubble.

Eq. (3) is a coupled nonlinear, second-order differential equation which can be reduced to two first-order differential equations. Applying Eq. (3) to each of the bubbles in the cluster, and using order reduction gives a system of $2N_{\text{bub}}$ first order differential equations as shown in Eq. (4) which can be solved numerically for the instantaneous bubble radii and wall velocities of every single bubble in the cluster.

$$\begin{bmatrix} 1 & 0 & 0 & 0 & \cdots & 0 \\ 0 & \left(1-\frac{\dot{R}_1}{c}\right)R_1+\frac{4\mu}{\rho c} & 0 & \frac{1}{s_{1,2}}R_2^2 & \cdots & \frac{1}{s_{1,N_{\text{bub}}}}R_{N_{\text{bub}}}^2 \\ 0 & 0 & \ddots & 0 & \cdots & \vdots \\ 0 & \frac{1}{s_{2,1}}R_1^2 & 0 & \ddots & \cdots & \frac{1}{s_{N_{\text{bub}}-1,N_{\text{bub}}}}R_{N_{\text{bub}}}^2 \\ \vdots & \vdots & \vdots & \vdots & 1 & 0 \\ 0 & \frac{1}{s_{N_{\text{bub}},1}}R_1^2 & \cdots & \frac{1}{s_{N_{\text{bub}},N_{\text{bub}}-1}}R_{N_{\text{bub}}-1}^2 & 0 & \left(1-\frac{\dot{R}_{N_{\text{bub}}}}{c}\right)R_{N_{\text{bub}}}+\frac{4\mu}{\rho c} \end{bmatrix}\begin{bmatrix} \dot{R}_1 \\ \ddot{R}_1 \\ \vdots \\ \vdots \\ \dot{R}_{N_{\text{bub}}} \\ \ddot{R}_{N_{\text{bub}}} \end{bmatrix}$$

$$=\begin{bmatrix} \dot{R}_1 \\ \left[-\frac{\dot{R}_1^2}{2}\left(3-\frac{\dot{R}_1}{c}\right)+\left(1+(1-3\kappa)\frac{\dot{R}_1}{c}\right)\left(\frac{P_0-P_v}{\rho}+\frac{2\sigma}{\rho R_{01}}\right)\left(\frac{R_{01}}{R_1}\right)^{3\kappa}-\frac{2\sigma}{\rho R_1}-\frac{4\mu\dot{R}_1}{\rho R_1}\right. \\ \left.-\sum_{j\neq i}^{N_{\text{bub}}}\frac{2}{s_{1,j}}R_j\dot{R}_j^2-\left(1+\frac{\dot{R}_1}{c}\right)\frac{P_0-P_v+\alpha\sin(2\pi f_{\text{ext}}t)}{\rho}-\frac{2\pi f_{\text{ext}}R_a\alpha}{\rho c}\cos(2\pi f_{\text{ext}}t)\right] \\ \vdots \\ \dot{R}_{N_{\text{bub}}} \\ \left[-\frac{\dot{R}_1^2}{2}\left(3-\frac{\dot{R}_1}{c}\right)+\left(1+(1-3\kappa)\frac{\dot{R}_1}{c}\right)\left(\frac{P_0-P_v}{\rho}+\frac{2\sigma}{\rho R_{01}}\right)\left(\frac{R_{01}}{R_1}\right)^{3\kappa}-\frac{2\sigma}{\rho R_1}-\frac{4\mu\dot{R}_1}{\rho R_1}\right. \\ \left.-\sum_{j\neq i}^{N_{\text{bub}}}\frac{2}{s_{1,j}}R_j\dot{R}_j^2-\left(1+\frac{\dot{R}_1}{c}\right)\frac{P_0-P_v+\alpha\sin(2\pi f_{\text{ext}}t)}{\rho}-\frac{2\pi f_{\text{ext}}R_a\alpha}{\rho c}\cos(2\pi f_{\text{ext}}t)\right] \end{bmatrix}. \tag{4}$$

3. Effects of bubble size

Ultrasound parameters of $\alpha = 40\,\text{kPa}$ and $f_{\text{ext}} = 100\,\text{kHz}$ are used for all simulations in this section, as they are commonly used in the literature [3,4,20]. Where bubble clusters are concerned, the inter-bubble distance is fixed at 50 μm,

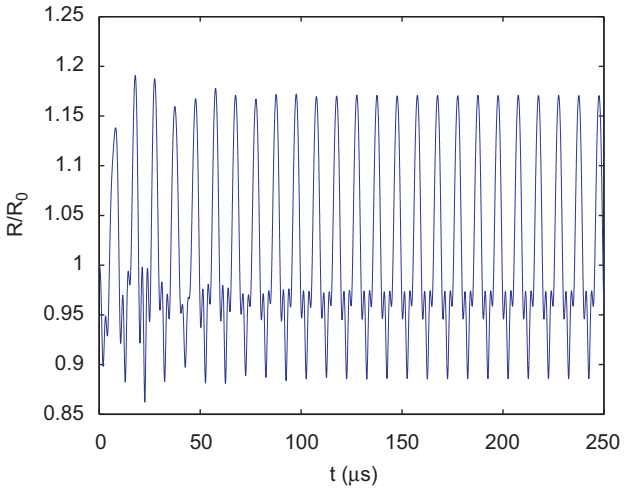

Fig. 1. Single bubble time response for $\alpha = 40\,\text{kPa}$, $f_{\text{ext}} = 100\,\text{kHz}$, $R_0 = 10\,\mu\text{m}$.

a value chosen such that no inter-bubble coalescence occurs for all cases considered, since bubble coalescence is not modelled in our mathematical formulation.

For most of our simulations, as Fig. 1 shows, the solutions goes through a transient period of typically around 100 μs followed by oscillations that is statistically stationary. In the subsequent analysis, only data from when the simulations are statistically stationary will be analysed. The maximum bubble expansion ratio at steady state, R_{max}/R_0, which can be determined from the phase diagrams, would be used as a measure of a bubble's amplitude of oscillations.

Table 1. summarizes all cases which would be considered in this section. Cases 1–3 are base cases for which the dynamics of an isolated bubble of different equilibrium radii are considered. An investigation of the bubble dynamics of a two-bubble cluster is attempted in cases 4 and 5. Case 4 examines how the addition of a slightly smaller bubble into the original system of a single bubble affects the dynamics of both bubbles, while case 5 considers the effect the addition of a considerably smaller bubble into the original system exerts on the dynamics of each bubble. Cases 6 and 7 investigate the same effects as cases 4 and 5, except that the bubble cluster size has been increased to $N_{bub} = 4$ to establish whether changing the number of bubbles in a cluster has an impact on the trend observed in cases 4 and 5.

Table 1
Summary of all simulation cases for the investigation of the effects of bubble size.

Case	N_{bub}	R_{01} (μm)	R_{02} (μm)	R_{03} (μm)	R_{04} (μm)
1	1	10	–	–	–
2	1	9	–	–	–
3	1	5	–	–	–
4	2	10	9	–	–
5	2	10	5	–	–
6	4	10	9	9	9
7	4	10	5	5	5

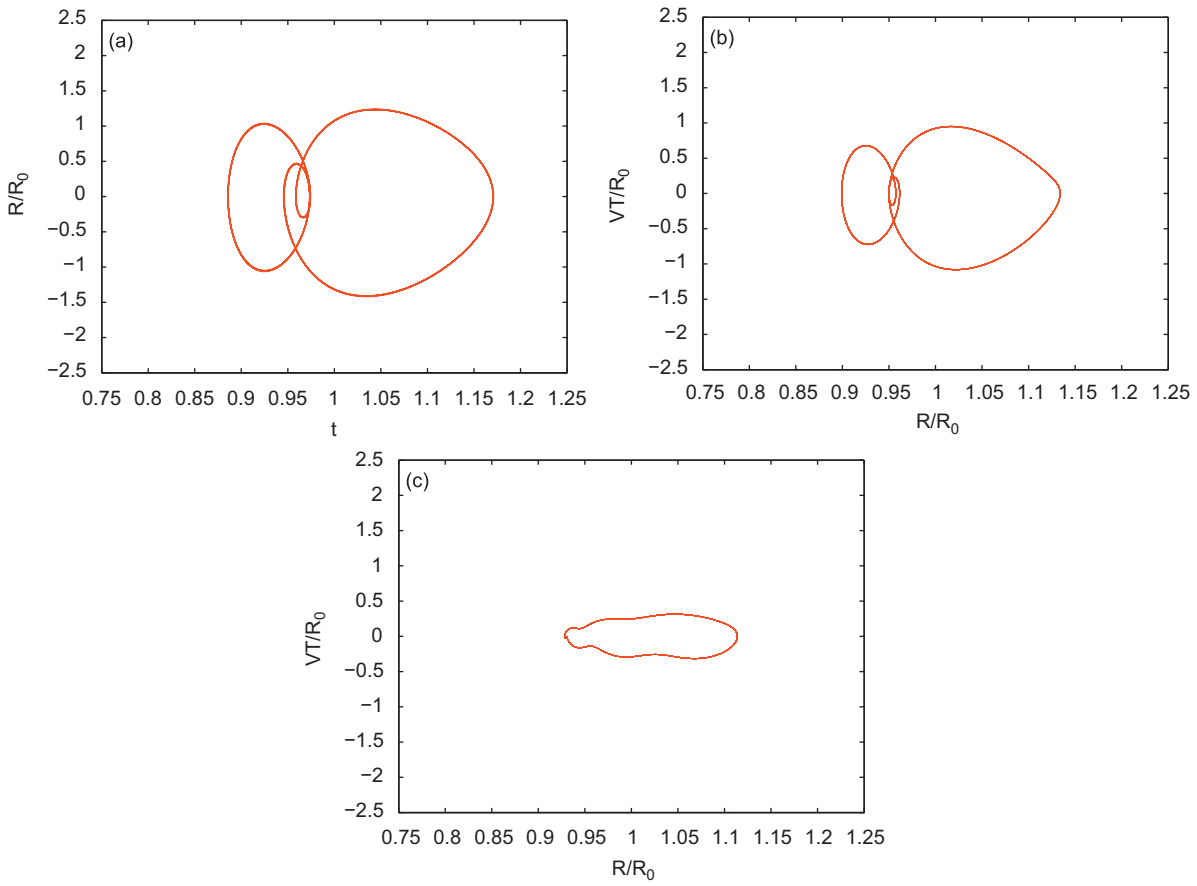

Fig. 2. Single bubble phase diagrams for $\alpha = 40$ kPa, $f_{ext} = 100$ kHz: (a) $R_0 = 10$ μm, (b) $R_0 = 9$ μm and (c) $R_0 = 5$ μm.

Fig. 2 shows the trajectory for a single bubble of three different equilibrium sizes, subject to the same set of ultrasound parameters of $\alpha = 40$ kPa and $f_{ext} = 100$ kHz. In the figure, $V = dR/dt$ is the bubble wall velocity and $T = 1/f_{ext}$ is the period of the external frequency. For $R_0 = 10\,\mu$m, the phase diagram of Fig. 2(a) reveals a crossing of bubble trajectories as the bubble returns to its original state in a single oscillation period. When a bubble that is 10 percent smaller is considered, the bubble performs an orbit with a general appearance similar to the previous case, accompanied by a slightly smaller amplitude of oscillation. However, when a bubble size which is 50 percent of the original size is used, it is apparent from Fig. 2 that a markedly different orbit with no intertwining results, and the amplitude of bubble oscillations is significantly reduced.

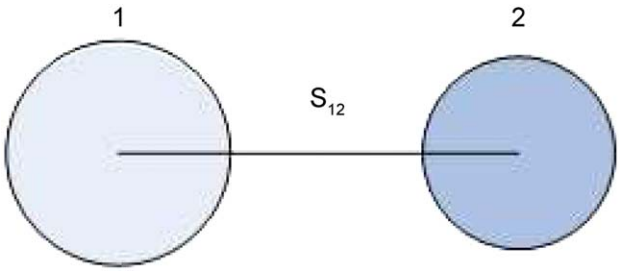

Fig. 3. Bubble arrangement and numbering for a cluster of two bubbles.

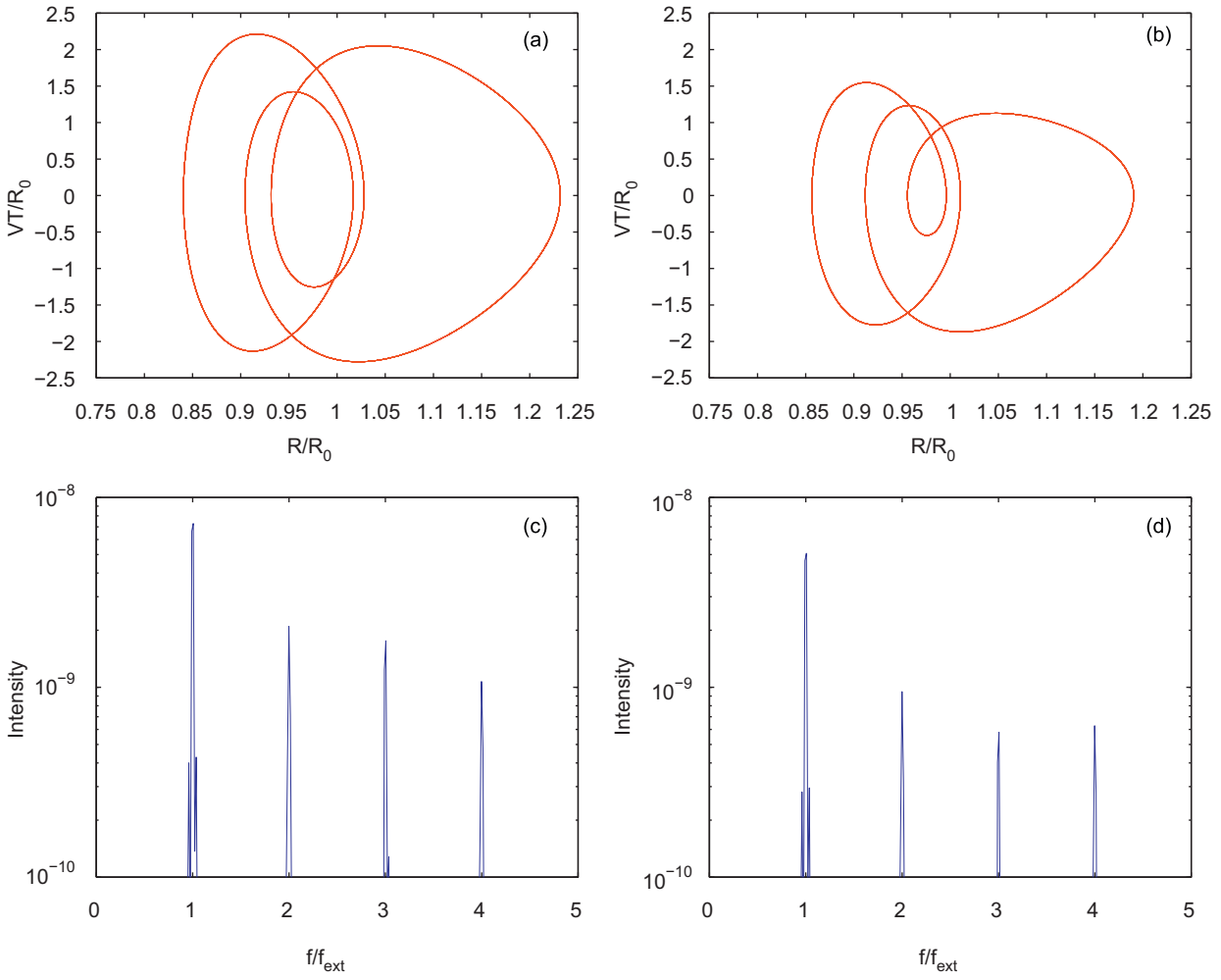

Fig. 4. Dynamical behaviour of bubbles for $N_{bub} = 2$, $\alpha = 40$ kPa, $f_{ext} = 100$ kHz, inter-bubble distance = 50 μm, $R_{01} = 10\,\mu$m, $R_{02} = 9\,\mu$m: (a) phase diagram of bubble 1, (b) phase diagram of bubble 2, (c) Fourier spectra of bubble 1, and (d) Fourier spectra of bubble 2.

A cluster of two microbubbles of different initial sizes arranged as in Fig. 3, subject to the same set of ultrasound parameters is then considered. Case 4, where one bubble is 10 percent smaller than other bubble in the cluster, and 5, where one bubble is 50 percent smaller than the other bubble in the cluster are examined.

The addition of one large-sized bubble into the original system of a single 10 μm bubble causes the phase diagrams of either bubble to differ from that of the single bubble case, as Figs. 4(a) and (b) clearly show. Furthermore, comparing Figs. 4(a) and (b) with Figs. 2(a) and (b), it can be observed that the amplitudes of oscillation for both bubbles are greater than that of the single bubble. This suggests that when there are two relatively large-sized bubbles in a system, each bubble contributes to the oscillation of the other bubble in the system via coupling. The degree of influence of a bubble on the dynamics of a neighbouring bubble in the system is in turn dependent on its equilibrium size; a hypothesis which will be investigated in the following simulation case. The frequency domain representation of the radius–time responses of Figs. 4(c) and (d) reveal that both bubbles are generating ultraharmonics at integer multiples of the driving frequency.

The addition of a relatively small-sized (5 μm) bubble into the original single large-sized (10 μm) bubble system yields virtually no effect on the dynamics of the 10 μm bubble, as the phase diagram of Fig. 5(a) matches that of Fig. 2(a) in terms of orbit pattern and bubble amplitude of oscillation. The state-space trajectory of the small-sized bubble in Fig. 5(b), has however been distorted from that of the single bubble of same size in Fig. 2(c). It appears that while the large-sized bubble has affected the dynamical behaviour of the smaller sized bubble, the smaller bubble has exerted minimal influence on the oscillations of the large bubble. This observation, together with the results of the previous simulation leads to the conclusion that the smaller the size of a bubble, the less influence it has on the dynamics of other bubbles in a cluster via its coupling terms. Comparing Fig. 5(c) with 4(c) and Fig. 5(d) with 4(d), it is clear that the magnitude of the ultraharmonics decreases with smaller bubble size.

The effects of bubble size on coupling is subsequently investigated for a cluster of four bubbles equidistant from each other, arranged as shown in Fig. 6. The same ultrasound parameters are used as before, and cases 6 and 7 as outlined in Table 1 are considered. Due to coupling symmetry, bubbles 2, 3 and 4 share the same dynamical behaviour for both cases.

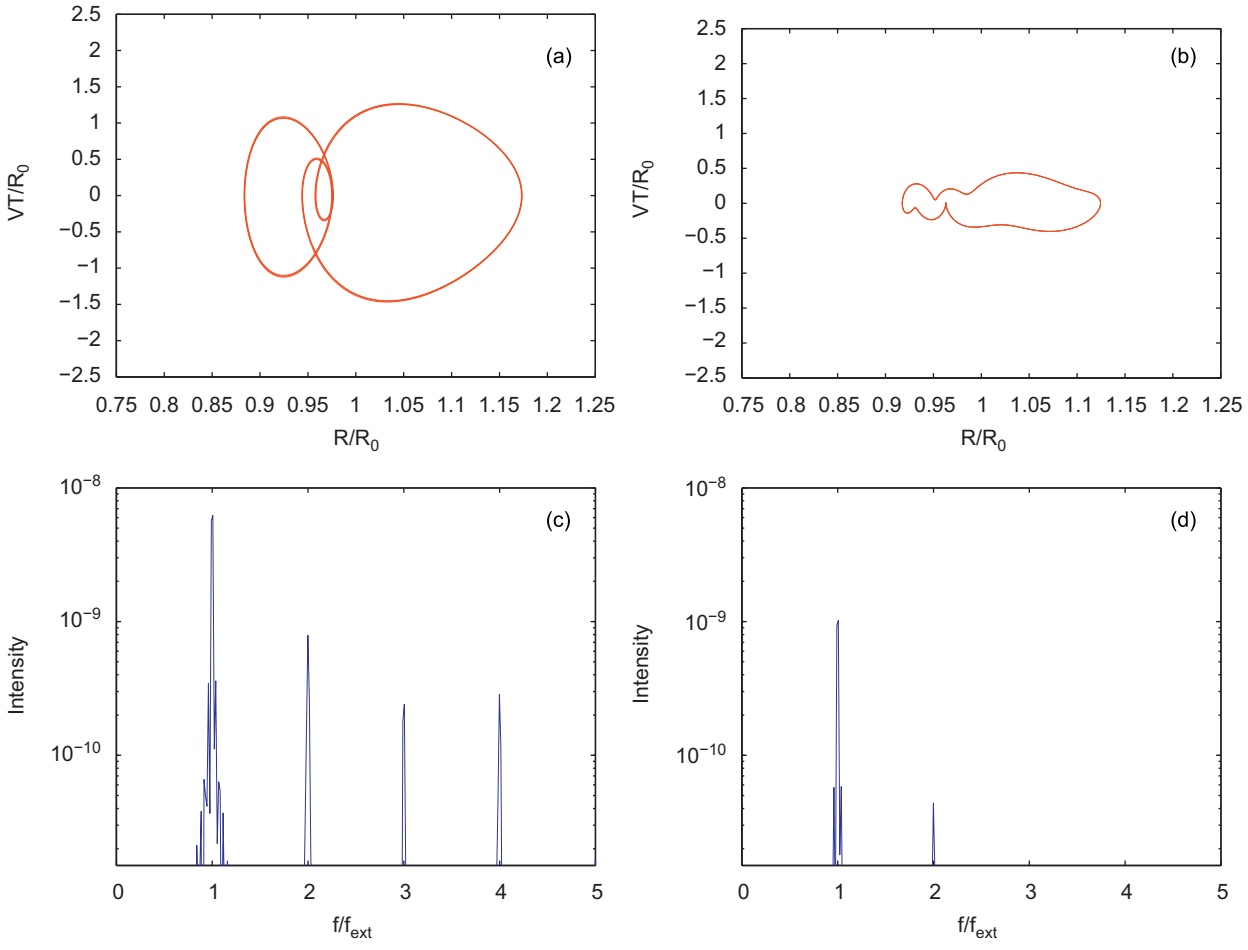

Fig. 5. Dynamical behaviour of bubbles for $N_{bub} = 2$, $\alpha = 40$ kPa, $f_{ext} = 100$ kHz, inter-bubble distance = 50 μm, $R_{01} = 10$ μm, $R_{02} = 5$ μm: (a) phase diagram of bubble 1, (b) phase diagram of bubble 2, (c) Fourier spectra of bubble 1, and (d) Fourier spectra of bubble 2.

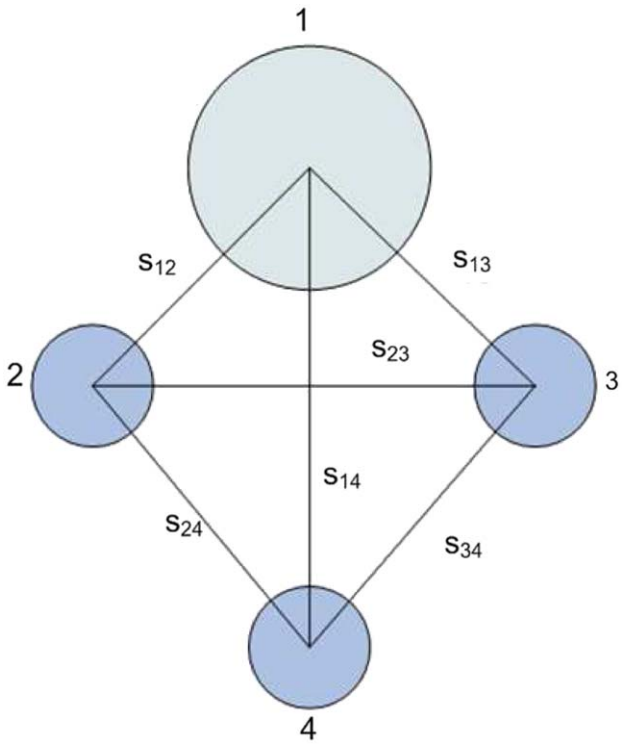

Fig. 6. Bubble arrangement and numbering for a cluster of four bubbles equidistant from each other.

When the sizes of bubbles in a cluster are not significantly different from each other, coupling drives the dynamical behaviour of any bubble to approach that of other bubbles in the cluster, as evidenced by the similarity of the phase portraits of Figs. 7(a) and (b). However, the phase portraits for this system resemble neither Fig. 2(a) nor 2(b), suggesting that coupling changes the dynamical behaviour of every bubble in a cluster from that of a single bubble considerably, particularly when all bubbles in the cluster are of a reasonably large size. The two major peaks appear at the main and third harmonics of the Fourier spectra for all bubbles, and the greater peak intensities of bubble 1 correlates with its greater amplitude of oscillation.

The trajectory of bubble 1, as seen from Fig. 8(a), bears a close resemblance to that of a single bubble of same size (Fig. 2(a)), when the other three bubbles in the cluster have half its equilibrium size. This observation, in addition to the dissimilarity in phase diagrams of the 5 μm bubble of Fig. 8(b) with that of the single, same-sized bubble case of Fig. 2(c) supports the conjecture that in a bubble cluster where bubbles of varying sizes interact with one other, larger sized bubbles exert a greater influence on the dynamics of neighbouring bubbles than smaller sized bubbles. Furthermore, the validity of this conclusion is unaffected by bubble cluster size, since the same trend in bubble dynamics is also observed in cases 4 and 5 where $N_{bub} = 2$. The Fourier spectra for bubble 1 differs from that of bubbles 2, 3 and 4 in that for the previous, a peak is generated at the second harmonic, which again contrasts with the previous simulation case ($R_{01} = 10\,\mu m$, $R_{02} = R_{03} = R_{04} = 9\,\mu m$) where the secondary peak for every bubble occurs at $f = 3f_{ext}$. These differences in acoustic signatures could potentially be utilized to distinguish between the various bubble sizes in a bubble cluster.

Comparing the Fourier spectra of Fig. 4 and those of Fig. 5, it can be observed that the magnitude of the ultraharmonic peaks of Figs. 4(c) and (d) have decreased when one of the bubbles in the two-bubble cluster is substituted for a smaller bubble with $R_0 = 5\,\mu m$, as evident in Figs. 5(c) and (d). Likewise, when three bubbles in the four-bubble cluster are replaced with three smaller bubbles of $R_0 = 5\,\mu m$, the ultraharmonic peaks at $f = 3f_{ext}$ of Figs. 7(c) and (d) have substantially decreased in Figs. 8(c) and (d). According to Lauterborn [20], ultraharmonics occur only when a certain acoustic pressure amplitude is exceeded, and this threshold pressure is raised to higher values for smaller bubble radii.

Fig. 9 shows how the maximum expansion ratio of bubble 1, which has a constant equilibrium size of $R_{01} = 10\,\mu m$, changes as size of other bubbles in a cluster of size $N_{bub} = 2$, 3 and 4, is varied from 3 to 10 μm, for ultrasound parameters of $\alpha = 40\,kPa$, $f_{ext} = 100\,kHz$. When the equilibrium sizes of other bubbles in the bubble cluster are relatively small, it is evident that changing the number of bubbles in a cluster has little effect on the maximum expansion ratio of the larger-sized bubble 1. A few peaks appear in the R_{max}/R_0 curves for each bubble cluster size, but main resonance peaks in the oscillation amplitude of bubble 1 are generated for larger neighbouring bubble sizes, which shifts to smaller neighbouring bubble sizes as the number of bubbles in the cluster is increased.

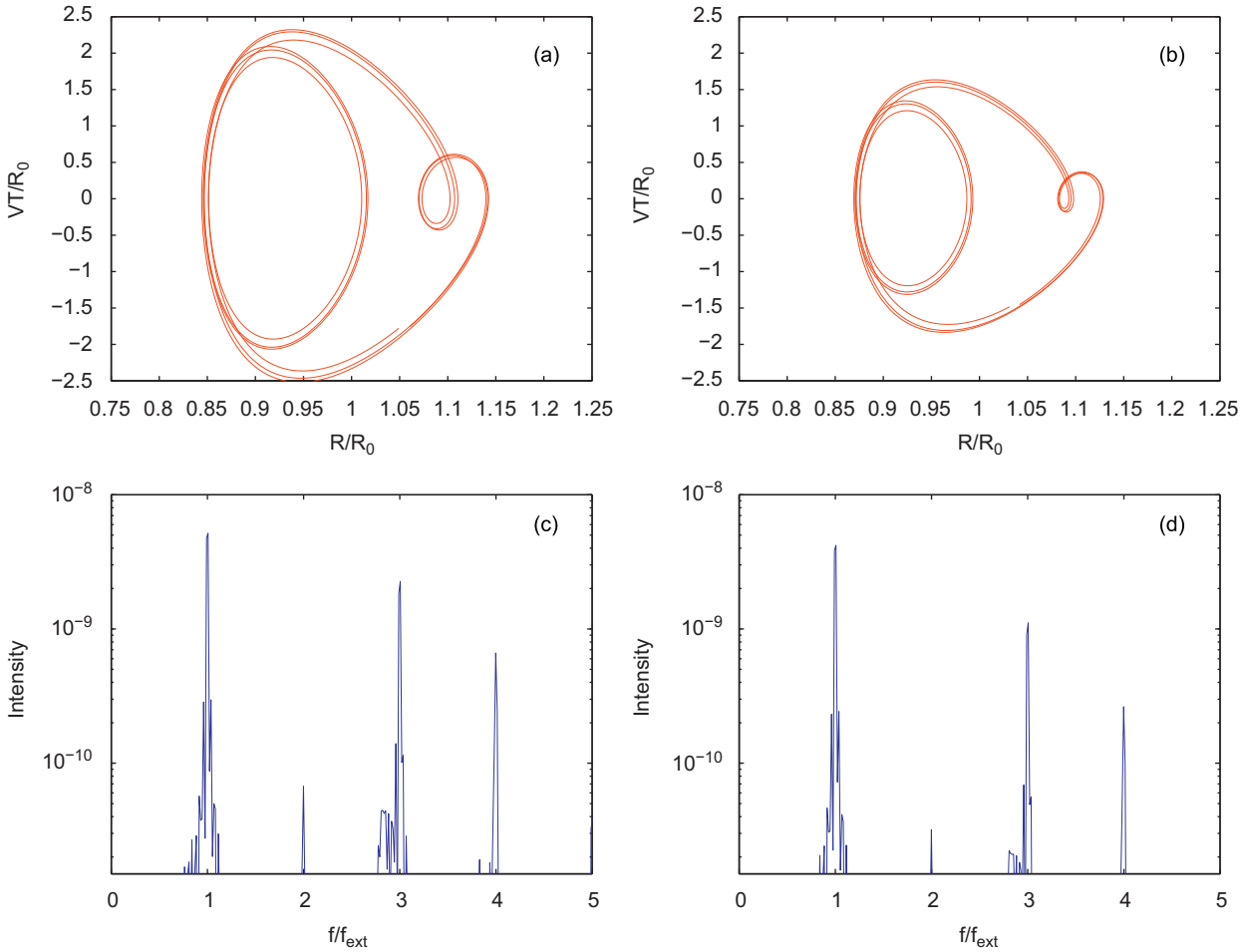

Fig. 7. Dynamical behaviour of bubbles for $N_{bub} = 4$, $\alpha = 40$ kPa, $f_{ext} = 100$ kHz, inter-bubble distance = 50 μm, $R_{01} = 10$ μm, $R_{02} = R_{03} = R_{04} = 9$ μm: (a) phase diagram of bubble 1, (b) phase diagram of bubbles 2, 3 and 4, (c) Fourier spectra of bubble 1, and (d) Fourier spectra of bubbles 2, 3 and 4.

4. Bifurcation characteristics

Using the bubble expansion ratio at every forcing period ($T = 1/f_{ext}$) from the stroboscopic maps as the state variable [4,13], the bifurcation diagrams were plotted at $f_{ext} = 1$ MHz as a function of driving pressure amplitude for a bubble cluster where all bubbles have (i) $R_0 = 10$ μm, (ii) $R_0 = 9$ μm and (iii) $R_0 = 5$ μm. The number of bubbles in the cluster is varied from $N_{bub} = 1$ to 4, and the inter-bubble distance is a constant 50 μm. In each individual case, since all bubbles have the same equilibrium radii and are equidistant from each other, a single bifurcation diagram applies to all bubbles in the structure.

For $R_0 = 10$ μm, the bifurcation diagram of Fig. 10(a) clearly reveals a period-tripling bifurcation at $\alpha \approx 160$ kPa. These three bifurcation branches extend up to $\alpha \approx 490$ kPa before merging and splitting into multiple points aligned vertically on the bifurcation diagram, indicating the existence of a multitude of frequencies of oscillation for the single bubble. This state of chaos, however, does not persist indefinitely, as a temporary transition from chaos to order for the system occurs at $\alpha \approx 540$ kPa, before reverting to chaos once again for slight increase in acoustic pressure amplitude. For greater driving pressure amplitudes, such intermittently chaotic behaviour occurs at $\alpha \approx 565$ and 650 kPa. A sevenfold increase in the period of oscillation occurs at $\alpha \approx 710$ kPa, leading the system towards full chaos for driving pressure amplitudes greater than 780 kPa.

The addition of one bubble of equal radius into the system changes the route to chaos for the system significantly. An inspection of Fig. 10(b) reveals that unlike the single bubble system, the two-bubble system does not follow a period-tripling route to chaos, but bubble oscillations become suddenly chaotic from an orderly, single-period oscillation at $\alpha \approx 480$ kPa. The first point of order-to-chaos transition for the two-bubble system is very close to that of the single bubble system, although their respective routes to this transition point differ considerably. Like the single bubble system, the

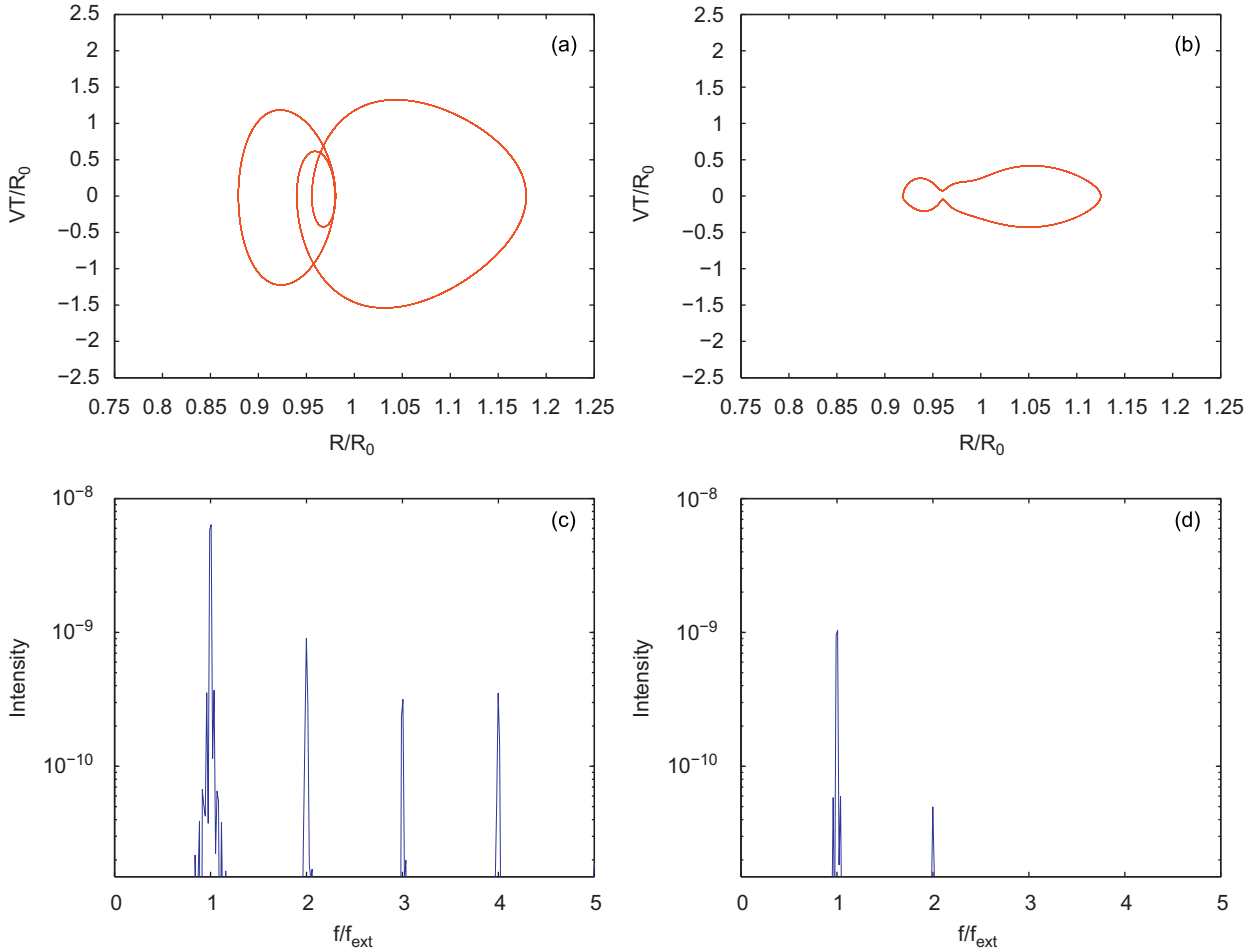

Fig. 8. Dynamical behaviour of bubbles for $N_{bub} = 4$, $\alpha = 40$ kPa, $f_{ext} = 100$ kHz, inter-bubble distance = 50 μm, $R_{01} = 10$ μm, $R_{02} = R_{03} = R_{04} = 5$ μm: (a) phase diagram of bubble 1, (b) phase diagram of bubbles 2, 3 and 4, (c) Fourier spectra of bubble 1, and (d) Fourier spectra of bubbles 2, 3 and 4.

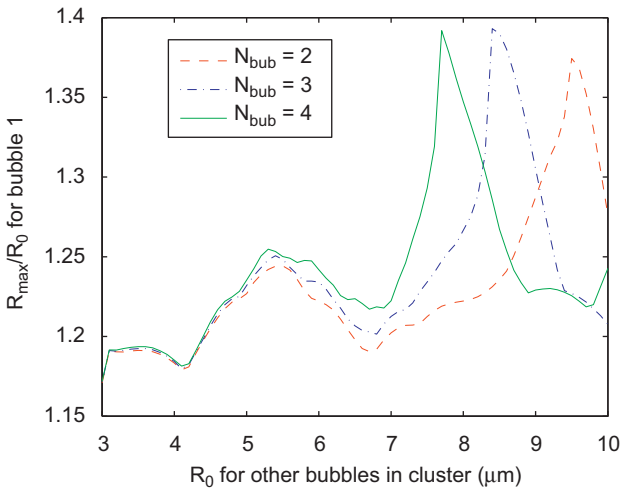

Fig. 9. R_{max}/R_0 for bubble 1 against R_0 of other equidistant bubbles in a cluster of different N_{bub} values, $R_{01} = 10$ μm, inter-bubble distance = 50 μm, $\alpha = 40$ kPa, $f_{ext} = 100$ kHz.

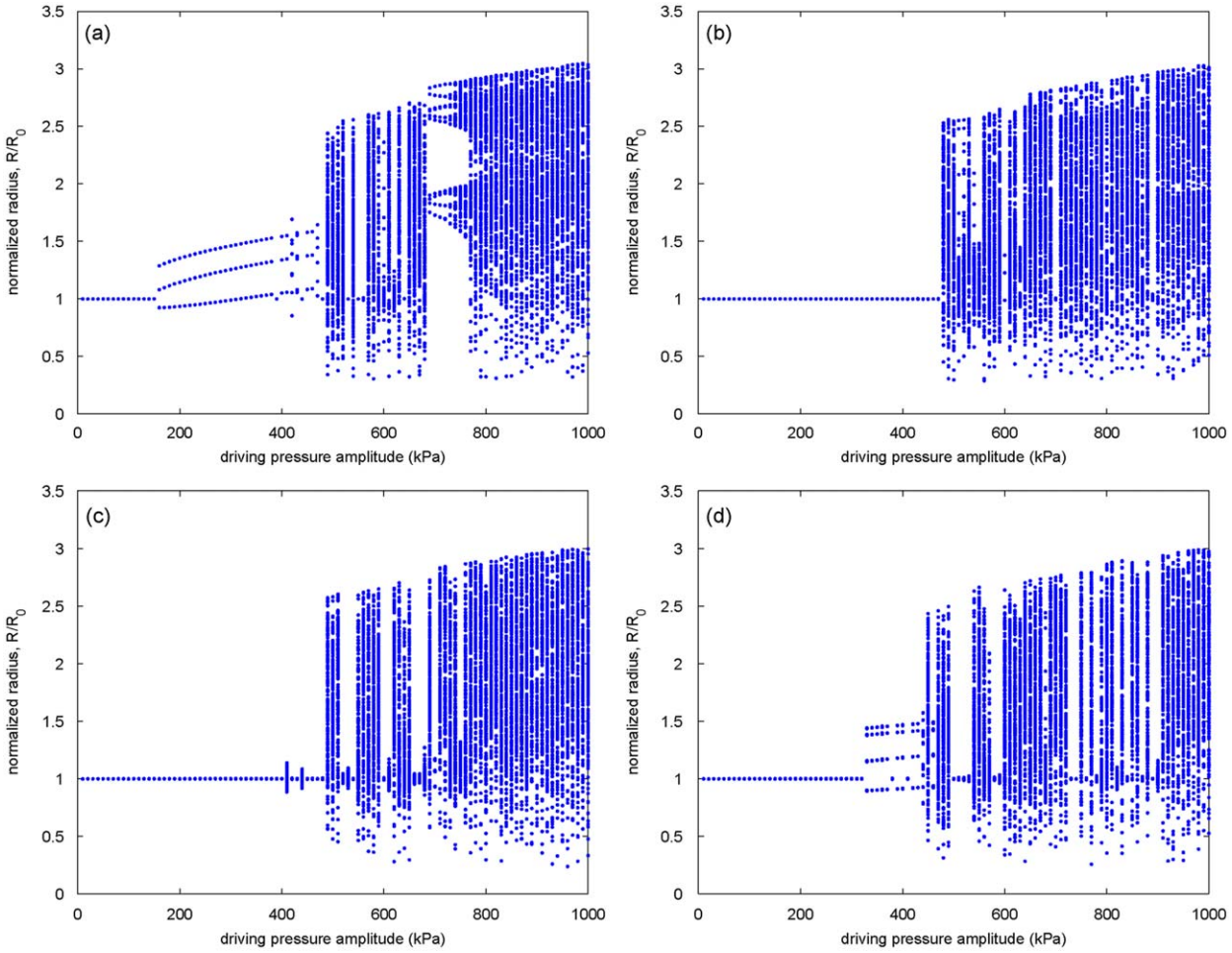

Fig. 10. Bifurcation diagrams at $f_{ext} = 1$ MHz, inter-bubble distance = 50 μm, $R_0 = 10$ μm for (a) $N_{bub} = 1$, (b) $N_{bub} = 2$, (c) $N_{bub} = 3$, (d) $N_{bub} = 4$.

two-bubble system encounters intermittent chaos at greater pressure amplitudes. Only one period-tripling bifurcation is observable for the two-bubble system at $\alpha \approx 600$ kPa.

The route to chaos of the three-bubble system does not differ much from that of the two-bubble system. The route to chaos for this system can still be classified as an intermittent one, as the bifurcation diagram of Fig. 10(c) does not feature any period-doubling or period-tripling cascades in the order-to-chaos pathway. However, in contrast to the previous two-bubble systems, the system first becomes chaotic at a lower pressure amplitude of $\alpha \approx 410$ kPa, but reverts to order once again for a slight increase in driving pressure amplitude. As in the previous two systems, 'windows of order', intervals for which the system switches from chaos to order, are observed in the chaotic, high pressure amplitude regions. The addition of one more bubble into the system changes the bifurcation characteristics of the bubbles rather dramatically. As can be seen in Fig. 10(d), the path to chaos of the bubble system evolves from an intermittent route to chaos to a period-quadrupling route to chaos classification. The first period-quadrupling cascade occurs at $\alpha \approx 325$ kPa, greater than the point of first bifurcation of the single-bubble case of Fig. 10(a). However, chaos is first encountered by this system at a smaller pressure amplitude of $\alpha \approx 430$ kPa. The various differences between the bifurcation diagrams of a single and two-bubble system expound the theory that bubble cluster size and coupling can affect a bubble's bifurcation characteristics and its route to chaos.

When $R_0 = 9$ μm, the single bubble system undergoes a period-tripling bifurcation like the single bubble of size $R_0 = 10$ μm. However, unlike the latter, each of the three bifurcation branches of the 9 μm bubble undergoes a further period-doubling bifurcation, causing the bubble to oscillate at $n/6$ multiples of the driving frequency, where $n = 1, 2, \ldots$. It is evident from Fig. 11(a) that the point of first bifurcation for this smaller bubble is also greater than that of the larger bubble of Fig. 10(a). The addition of one bubble of equal size into the system still results in a period-tripling bifurcation. The pressure amplitude for which this bifurcation first occurs has, however, shifted to a smaller value of $\alpha \approx 175$ kPa. A 'window of order' can still be observed at high pressure amplitudes of $930\text{ kPa} < \alpha < 990$ kPa. When one more bubble is

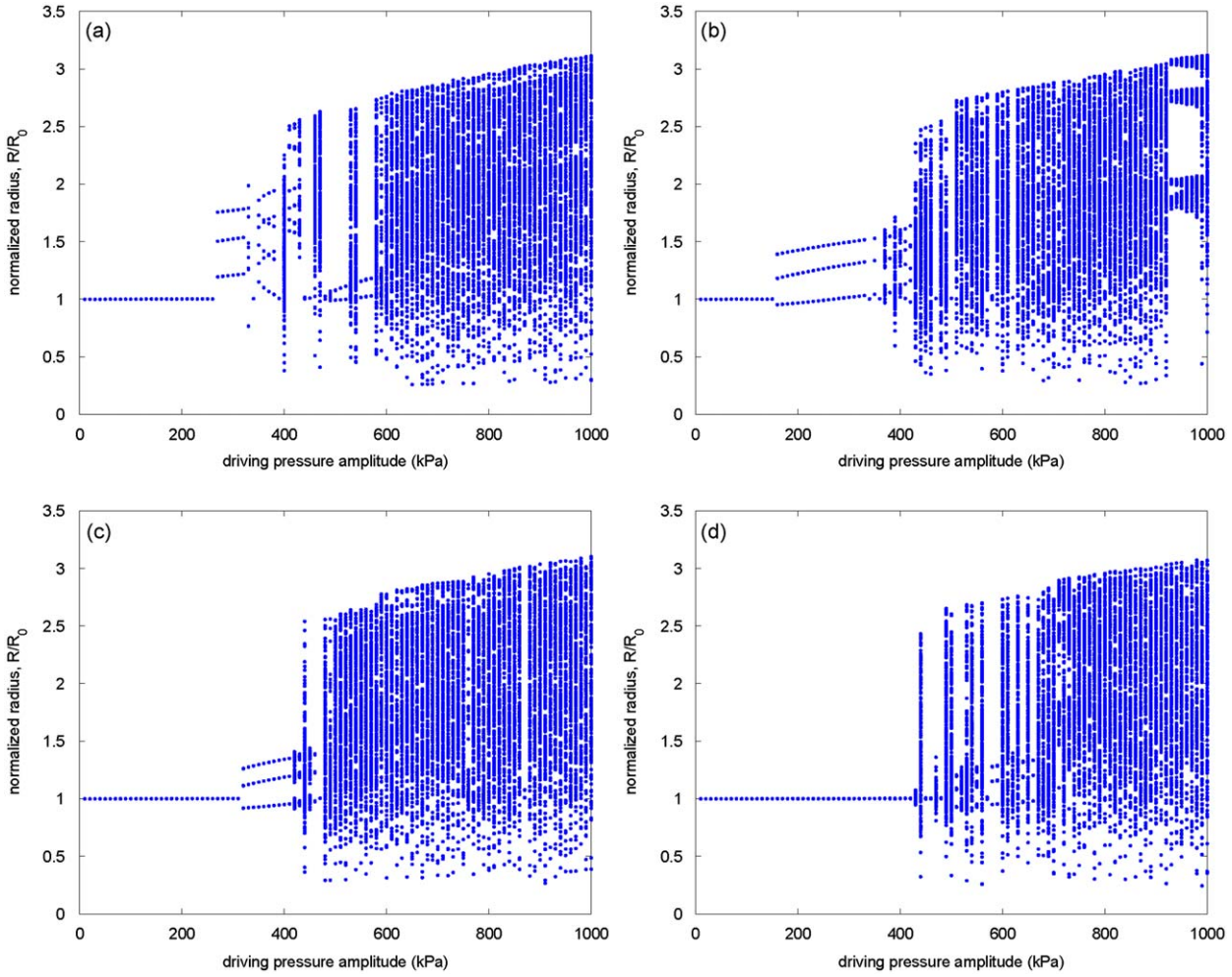

Fig. 11. Bifurcation diagrams at $f_{ext} = 1$ MHz, inter-bubble distance = 50 μm, $R_0 = 9$ μm for (a) $N_{bub} = 1$, (b) $N_{bub} = 2$, (c) $N_{bub} = 3$, (d) $N_{bub} = 4$.

added into the system, the point of first bifurcation of the bubbles does not shift downwards as expected, but increases to a much greater value of $\alpha \approx 320$ kPa as Fig. 11(c) illustrates. When $N_{bub} = 4$, there is a change in the bubble system's route to chaos. The bubble system no longer undergoes a bifurcation in its route to chaos. A transition from chaos to a period-tripling bifurcation, however, occurs at $\alpha \approx 570$ kPa, before reverting to chaos once again at $\alpha \approx 600$ kPa.

Unlike bubbles of 9 and 10 μm equilibrium radii in the previous simulation cases, a single 5 μm bubble takes a classical period-doubling route to chaos, as Fig. 12(a) reveals. When one bubble is added into the system, the route to chaos of the system is not altered. However, the point for which the system first undergoes bifurcation and the transition acoustic pressure at which the system descends into full chaos are shifted to lower values. For $N_{bub} = 3$, the bubble system first experiences a period-doubling at $\alpha \approx 170$ kPa, followed by a saddle-node bifurcation for a small increase in pressure amplitude. The destruction of a stable limit cycle and the birth of a new one is characterized by a discontinuous jump in bubble expansion ratio as seen in the bifurcation diagram of Fig. 12(c). The addition of one bubble to the three-bubble cluster results in a simultaneous period-doubling and saddle-node bifurcation at a lower pressure amplitude of $\alpha \approx 150$ kPa. Like the three-bubble system, the four-bubble cluster undergoes a chaos-to-order transition at higher pressures, but the range of acoustic pressure amplitudes for which chaos is experienced is wider for the four-bubble cluster.

The effects of coupling are complicated, as they add to the degree of non-linearity of the pre-existing, highly non-linear system modelled by the Keller–Miksis–Parlitz equation. However, it is apparent from the results of this section that coupling plays an important role in reducing a bubble system's degree of chaos. This is a very useful result, as it demonstrates that chaotic oscillations may be suppressed according to how many bubbles are present in a cluster, as an alternative to the dual forcing frequency approach highlighted by [21]. An observable trend, however, exists for changing bubble size. Comparing the bifurcation diagrams of Figs. 10–12, there is evidence that a small bubble cluster consisting of smaller-sized bubbles transitions from order to chaos at lower driving pressure amplitudes.

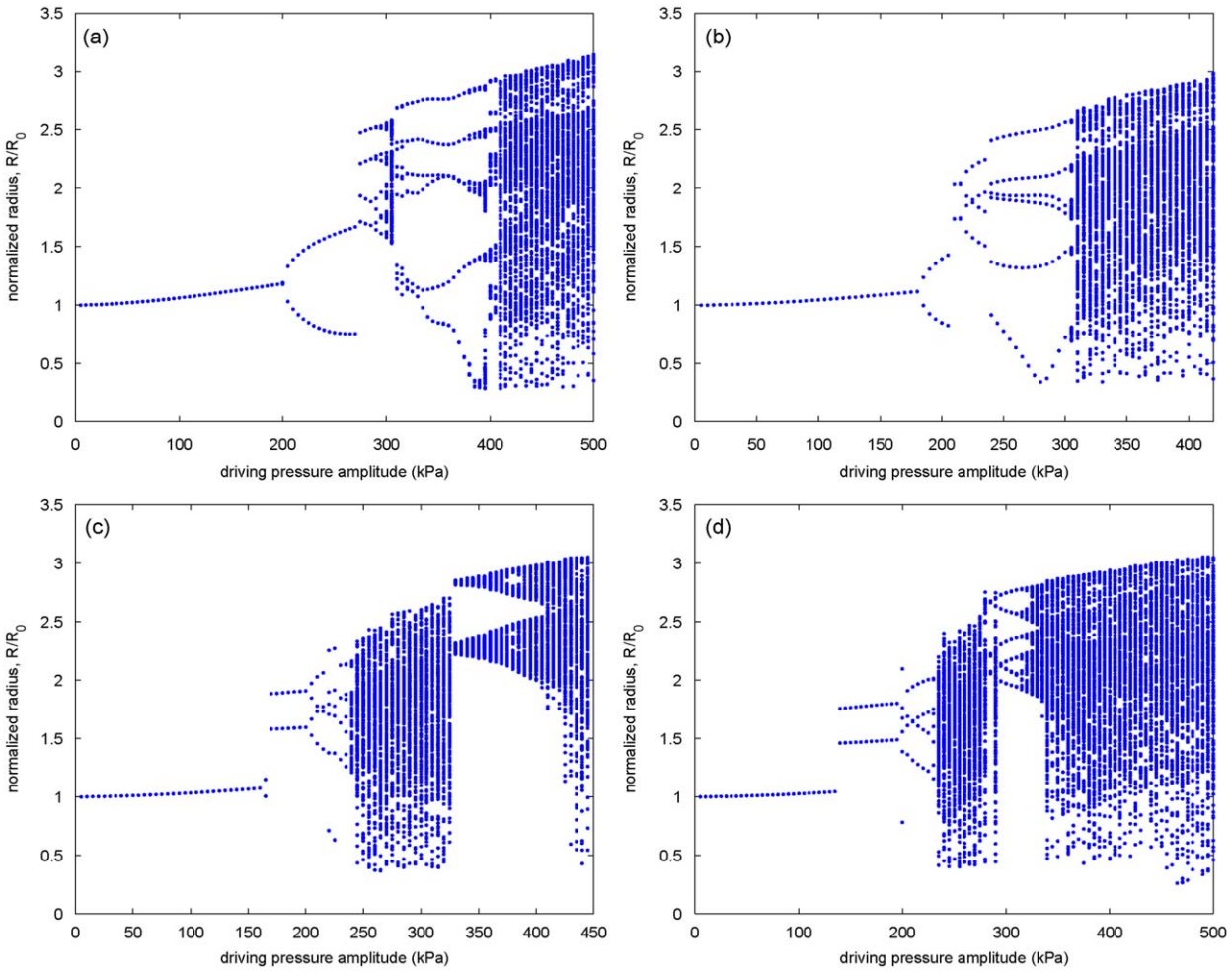

Fig. 12. Bifurcation diagrams at $f_{ext} = 1$ MHz, inter-bubble distance = 50 μm, $R_0 = 5$ μm for (a) $N_{bub} = 1$, (b) $N_{bub} = 2$, (c) $N_{bub} = 3$, (d) $N_{bub} = 4$.

5. Conclusion

A theoretical model was implemented for predicting the dynamics of a bubble cluster of any size, within which each bubble may assume different initial conditions from other bubbles in the cluster. Numerical simulations were performed, and it was found that coupling can alter a bubble cluster's bifurcation characteristics and route to chaos. The possibility of suppressing the chaotic oscillations of microbubbles by varying bubble cluster size exists. Also, it was discovered that a small bubble cluster consisting of smaller-sized bubbles transitions from order to chaos at lower driving pressure amplitudes. In addition, it was found that larger bubbles influence the dynamics of smaller bubbles in a cluster more than smaller bubbles do.

References

[1] C.E. Brennen, *Cavitation and Bubble Dynamics*, Oxford University Press, New York, 1995.
[2] W.L. Nyborg, Biological effects of ultrasound: development of safety guidelines-part II: general review, *Ultrasound in Medicine and Biology* 27 (2001) 301–333.
[3] J.B. Keller, M. Miksis, Bubble oscillations of large amplitude, *The Journal of the Acoustical Society of America* 68 (1980) 628–633.
[4] U. Parlitz, V. Englisch, C. Scheffczyk, W. Lauterborn, Bifurcation structure of bubble oscillators, *The Journal of the Acoustical Society of America* 88 (1990) 1061–1077.
[5] A. Doinikov, Mathematical model for collective bubble dynamics in strong ultrasound fields, *The Journal of the Acoustical Society of America* 116 (2004) 821–827.
[6] R. Manasseh, A. Nikolovska, A. Ooi, S. Yoshida, Anisotropy in the sound field generated by a bubble chain, *Journal of Sound and Vibration* 278 (2004) 807–823.
[7] A. Doinikov, R. Manasseh, A. Ooi, On time delays in coupled multibubble systems, *Journal of the Acoustical Society of America* 117 (2005) 47–50.

[8] E. Payne, S. Illesinghe, A. Ooi, R. Manasseh, Symmetric mode resonance of bubbles attached to a rigid boundary, *Journal of the Acoustical Society of America* 118 (2005) 2841–2849.
[9] A. Nikolovska, R. Manasseh, A. Ooi, On the propagation of acoustic energy in the vicinity of a bubble chain, *Journal of Sound and Vibration* 306 (2007) 507–523.
[10] A. Ooi, A. Nikolovska, R. Manasseh, Analysis of time delay effects on a linear bubble chain system, *Journal of the Acoustical Society of America* 124 (2008) 815–826.
[11] A. Ooi, R. Manasseh, Coupled nonlinear oscillations of microbubbles, *Australian & New Zealand Industrial and Applied Mathematics Journal* 46E (2005) C102–C116.
[12] W. Lauterborn, A. Koch, Holographic observation of period-doubled and chaotic bubble oscillations in acoustic cavitation, *Physical Review A* 35 (1987) 1974–1976.
[13] W. Lauterborn, U. Parlitz, Methods of chaos physics and their application to acoustics, *The Journal of the Acoustical Society of America* 84 (1988) 1975–1993.
[14] J.S. Allen, D.E. Kruse, P.A. Dayton, K.W. Ferrara, Effect of coupled oscillations on microbubble behaviour, *The Journal of the Acoustical Society of America* 114 (2003) 1678–1690.
[15] V. Garbin, B. Dollet, M.L.J. Overvelde, N. de Jong, D. Lohse, M. Versluis, D. Cojoc, E. Ferrari, E. Fabrizio, Coupled dynamics of an isolated UCA microbubble pair, *2007 IEEE Ultrasonics Symposium*, 2007, pp. 757–760.
[16] C.A. Macdonald, J. Gomatam, Chaotic dynamics of microbubbles in ultrasonic fields, *Journal of Mechanical Engineering Science-Proceedings of IMechE (Part C)* 220 (2006) 333–343. DOI:10.1243/095440606X79596.
[17] H. Takahira, S. Yamane, T. Akamatsu, Nonlinear oscillations of a cluster of bubbles in a sound field, *The Japan Society of Mechanical Engineers Series B* 38 (1995).
[18] R. Mettin, I. Akhatov, U. Parlitz, C.D. Ohl, W. Lauterborn, Bjerknes forces between small cavitation bubbles in a strong acoustic field, *Physical Review E* 56 (1997) 2924–2931.
[19] M. Ida, A characteristic frequency of two mutually interacting gas bubbles in an acoustic field, *Physics Letters A* 297 (2002) 210–217.
[20] W. Lauterborn, Numerical investigation of nonlinear oscillations of gas bubbles in liquids, *The Journal of the Acoustical Society of America* 59 (1976) 283–293.
[21] S. Behnia, A. Jafari, W. Soltanpoor, O. Jahanbakhsh, Possibility of using dual frequency to control chaotic oscillations of a spherical bubble, Arxiv preprint arXiv:0801.1949, 2008.